# Spatial Profiles of Stimulated Brillouin Scattering Ion Waves in a Laser-Produced Plasma

P. E. Young

*University of California, Lawrence Livermore National Laboratory, P.O. Box 5508, Livermore, California 94550*

(Received 13 July 1994)

The ion fluctuation axial profile is measured by Thomson scattering in an inhomogeneous laser-produced plasma. The electron temperature and plasma drift velocity at the location of the measured ion waves and the plasma density profile are simultaneously measured. The measured ion fluctuation profile is compared to the profile predicted by convective growth of the stimulated Brillouin scattering instability calculated from the measured hydrodynamic profiles.

PACS numbers: 52.35.Fp, 52.35.Mw, 52.40.Nk, 52.50.Jm

Stimulated Brillouin scattering (SBS) is a parametric instability in a plasma in which an electromagnetic wave interacts with an ion acoustic wave to produce a scattered electromagnetic wave [1–5]. SBS has been a concern in inertial confinement fusion (ICF) applications as a potential cause of decreased laser-target coupling efficiency. The instability continues to be of interest in a scientific sense because the seeding and saturation mechanisms are not well understood. Although Thomson scattering [6,7] has been used extensively to identify ion waves in interactions between plasmas and 10.6 $\mu$m wavelength lasers [8,9], the plasma and laser parameters for ICF targets will be substantially different. SBS in short-wavelength laser-plasma interactions has been studied via scattered light spectra near the incident laser wavelength, and, although there has recently been evidence of seeding of SBS by the two-plasmon decay (TPD) instability at $n_c/4$ [10], the interpretation of spectra is confused by the role of the (unknown) expansion velocity profile. Applications [11,12] of convective gain theory have shown its difficulty in predicting the spectra and signal levels of experiments.

In this Letter, we discuss an experiment in which we have determined both the plasma hydrodynamic profiles and the ion acoustic fluctuation profile (using the Thomson scattering technique) in a plasma produced by a laser with a wavelength, $\lambda_o$, of 1.064 $\mu$m irradiating a solid carbon target. This means that, for the first time, we can compare an experimental ion wave fluctuation spatial profile to a theoretically predicted one. We find that the spatial dependence and quantitative level of the density fluctuations are adequately modeled for densities above $n_c/4$ by convective gain theory, provided the instability is assumed to grow from laser light scattering from ion acoustic fluctuations. Although Thomson scattering from SBS ion waves has been observed before, this was done in $CO_2$ laser produced plasmas which have significantly different hydrodynamic profiles, and, in general, the instability is strongly coupled whereas most theory to date has assumed weak coupling. Also, the emphasis in those experiments was on measuring growth rates of SBS.

The experiment was conducted using the Janus laser facility at the Lawrence Livermore National Laboratory. The plasma was produced using a 1 ns full width at half maximum Gaussian laser pulse ($\lambda_o = 1.064$ $\mu$m) which irradiated a solid carbon target. The laser spatial profile is nominally square topped (the measured profile is shown in Ref. [13]). A laser energy of 50 J and a spot diameter of 250 $\mu$m produced an average laser intensity on target of $1 \times 10^{14}$ W/cm$^2$. The laser intensity is intentionally kept low in order to satisfy the condition for weak coupling [4,5] between the pump wave and the ion acoustic wave. The instability is weakly coupled when $\gamma_0 \ll k_{ia} c_s$, where $\gamma_0$ is the SBS growth rate, $k_{ia}$ is the ion acoustic wave number, and $c_s$ is the sound speed.

Thomson scattering [14] was used to make local measurements of the ion fluctuation level. The probe beam was of wavelength 0.35 $\mu$m, of 1 ns duration, was incident at an angle of 45° with respect to the laser axis, and scattered light was collected at an angle 90° from the probe axis and 45° from the laser axis; the probe beam, laser beam, and collector axis were all in the same plane. The angles were chosen to maximize the scattered signal from ion acoustic waves with a wave number of $2k_0$; this is the predicted wave number for maximum growth of SBS in direct backscatter [3,4]. Calibration of the diagnostic showed that the scattered light was collected from a spherical volume of $<50$ $\mu$m in diameter. Profiles of the ion fluctuations along the laser axis (axis of expansion) were obtained over a series of laser pulses by scanning the positions of the target and the focal lens relative to the scattering volume. The incident laser energy of each pulse is kept within 10% of the energy averaged over all the pulses. The collected signal was relayed to an optical streak camera with an S-20 photocathode which provided time resolution ($\simeq$50 ps); interference filters defined a bandpass of $\pm$50 Å about the probe wavelength with $10^4$ rejection of wavelengths outside this spectral region.

The target was imaged onto the input slit of the streak camera so that the streak record had time as one dimension and space in the orthogonal dimension. This allowed us to mask the image in such a way as to eliminate any probe light that is specularly reflected from the target. In addition, we verified that the signal was caused by light scattered from parametrically driven waves by probing after the pump laser turned off and observing no signal. Similarly, no signal was observed prior to the arrival of

0031-9007/94/73(14)/1939(4)$06.00  

the plasma forming beam. A timing fiducial allows us to match the SBS scattered signal to the probe and the laser. In the experiment described here, the peak of the probe pulse coincided in time with the peak of the main pulse.

The measured scattered signal can be related to the density fluctuation level $\tilde{n}$. If the scattering takes place from a coherent ion acoustic wave, then the fluctuation level is proportional to the square root of the scattered power level [8,14]:

$$(\tilde{n}/n_e)^2 = 4dP_s/\pi d\Omega P_i n_e^2 r_e^2 L_z^2 a_0^2, \quad (1)$$

where $dP_s$ is the power that is Thomson scattered into the solid angle $d\Omega$ (= 0.05 sr), $P_i$ is the incident probe power (= $10^9$ W), $r_e$ is the classical electron radius (= $2 \times 10^{-13}$ cm), $L_z$ is the path length of the probe beam through the scattering volume (= 50 $\mu$m), and $a_0$ is the radius of the incident probe beam (= 25 $\mu$m). The scattered power was estimated both by measuring the light scattered from a glass target and by comparison to the fiducial signal level.

Figure 1 shows the scattered SBS signals from five different spatial positions as a function of time. For the measurements at the position $z$ = 100 $\mu$m, corresponding to the highest probed density, there is a signal only for a short time near the peak of the laser pulse. For distances farther from the target, the signals are stronger after the peak of the laser pulse, which is consistent with the development of longer gradient scale lengths at later times. From Eq. (1), we calculate a maximum $\tilde{n}/n_e \simeq 3 \times 10^{-4}$.

Thomson scattering also provides a measurement of the electron temperature and the expansion velocity [6,7]. The spectrum of the probe beam light scattered 90° to the plane of the incident probe beam and the 1.06 $\mu$m plasma forming beam is recorded with a streak camera. We observe double-peaked features associated with ion acoustic fluctuations, and an example of the signal at the peak of the probe pulse and $z$ = 200 $\mu$m is shown in Fig. 2. The wavelength separation of the peaks is dependent on the electron temperature, with a frequency difference of $\Delta\omega = 2\Delta k c_s$ where $\Delta k = \sqrt{2}k_0$ is the wave number of the ion acoustic fluctuation that is doing the scattering (determined by the probe-collection geometry). The wavelength shift of the peaks relative to the incident probe wavelength is dependent on the Doppler shift of the probe by the plasma flow in the scattering volume.

The result of a spatial scan of the electron temperature and the flow velocity at the peak of the laser pulse is shown in Fig. 3(a). The plasma is nearly isothermal, as expected.

An interferogram was also recorded on each laser pulse (see Fig. 4). The interferometer was of the folded wave type, and the probe beam was 30 ps Gaussian, 0.35 $\mu$m, and timed to occur at the middle of the laser pulse. The target is imaged onto a television camera which is used to record the interferogram. The interferogram without the plasma consists of parallel reference fringes across the field of view. Introduction of a plasma bends the fringes towards the right in Fig.4, and one fringe shift relative to

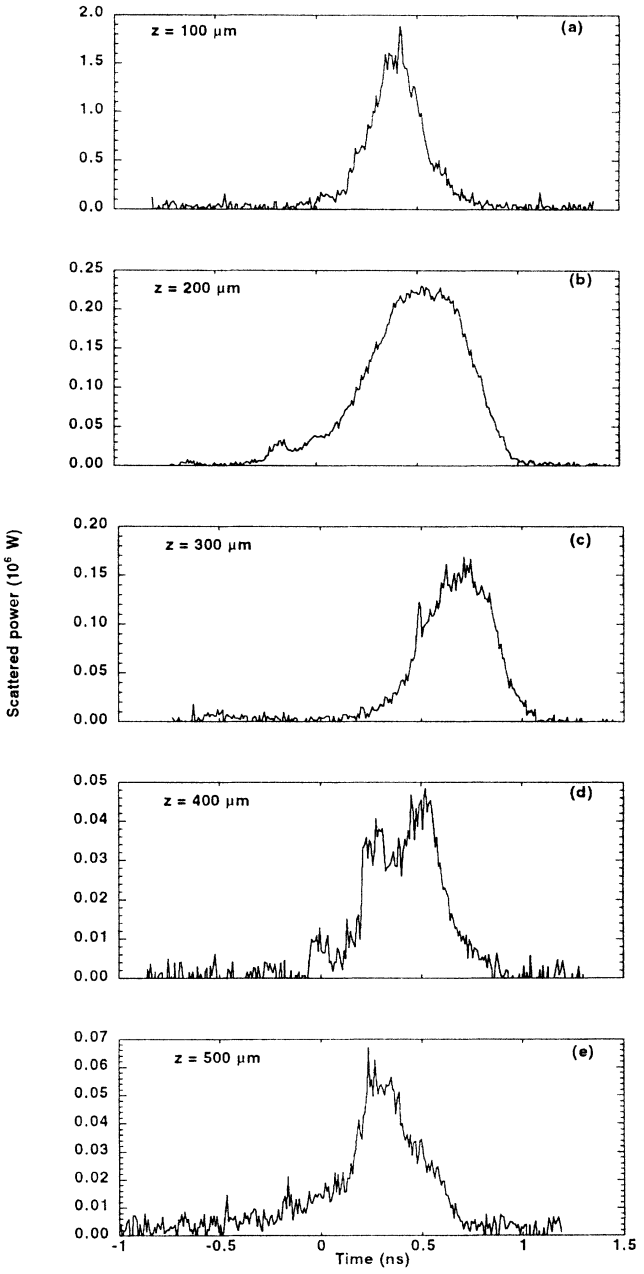


FIG. 1. The Thomson scattered signals from SBS ion waves are obtained at distances of (a) 100, (b) 200, (c) 300, (d) 400, and (e) 500 $\mu$m from the target surface on different target irradiations.

the background fringe corresponds to a $2\pi$ phase shift. The phase shift is related to the plasma density by

$$\delta\phi = 9 \times 10^{-22} L_{p,\mu} \lambda_{p,\mu} n_e, \quad (2)$$

where $L_{p,\mu}$ is the probe beam path length through the plasma (in microns), and $\lambda_{p,\mu}$ is the probe beam wavelength (in microns). The interferogram provides a record of the pulse-to-pulse variation of the plasma, and for any particular pulse we can Abel invert the interferogram to obtain the plasma density profile along the laser axis [see Fig.3(b)].

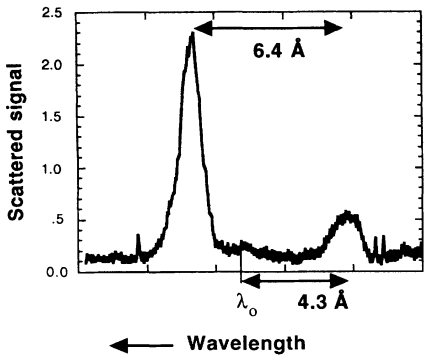


FIG. 2. The Thomson scattered signal obtained for the $T_e$ measurement is shown in this figure. The wavelength separation of the peaks corresponds to $T_e = 1.0$ keV, and the shift of the peaks relative to $\lambda_0$ corresponds to a flow velocity of $2 \times 10^7$ cm/s.

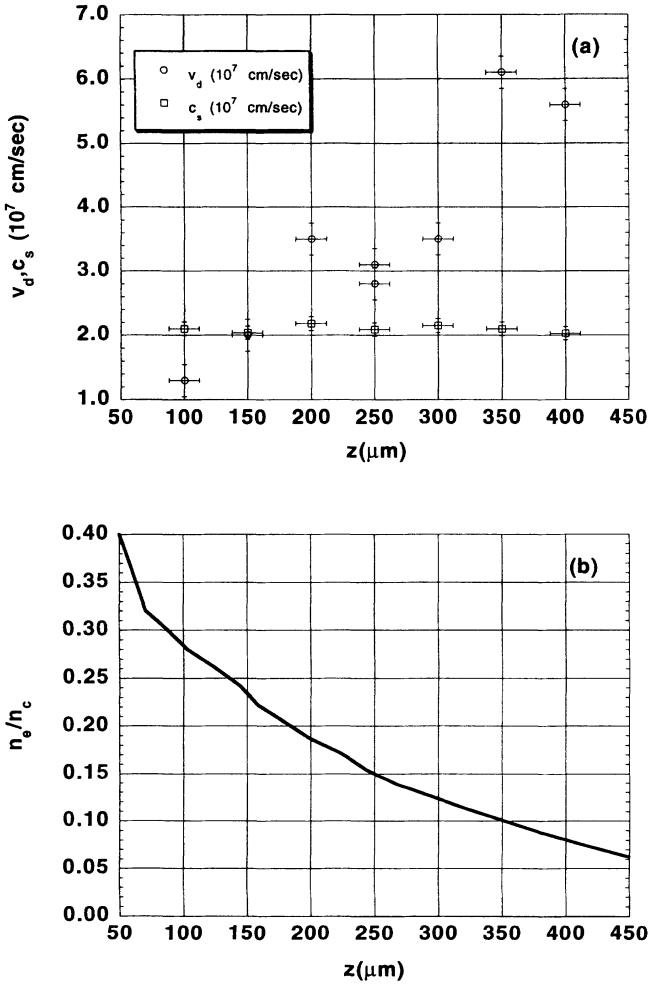


FIG. 3. The hydrodynamic profiles have been experimentally measured. (a) The density profile has been obtained by inverting the interferogram shown in Fig. 4. (b) The expansion velocity and the sound speed profiles are measured at the peak of the laser pulse.

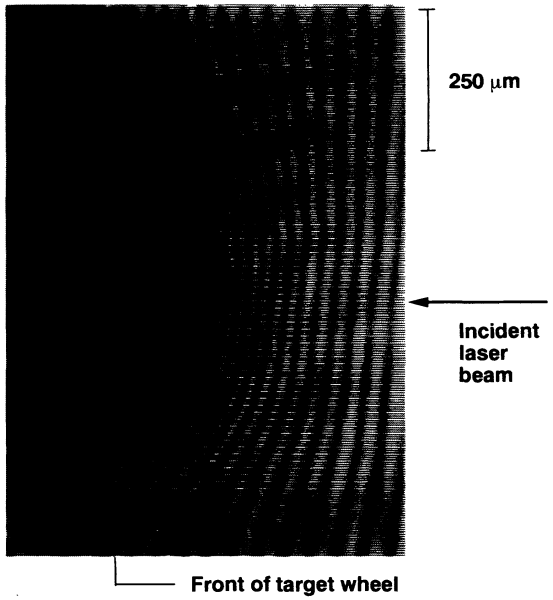


FIG. 4. The interferograms are recorded at the peak of the laser pulse by a 30 ps, 0.35 $\mu$m probe pulse. The shadow of the target wheel is shown. The Thomson scattered signal for the $T_e$ measurement is collected by a lens located below the target wheel in this picture.

Convective gain theory predicts that the SBS instability grows from the initial fluctuation level by $e^G$, where $G$ is the direct backscattering convective gain given by [see Eq. (7) of Ref. [5]]:

$$G \sim \frac{\frac{1}{8}\left(\frac{v_0}{v_e}\right)^2 \frac{n}{n_c}\frac{\omega_0}{c} L_u}{\left|\frac{L_u}{L_n}\frac{n}{n_c}(1-M) - 2\left(1-\frac{n}{n_c}\right)\left(1-\frac{L_u}{L_T}\right)\right|}, \quad (3)$$

where $v_0$ is the electron quiver velocity, $v_e$ is the electron thermal velocity, and $L_n = n_e(dn_e/dx)^{-1}$, $L_T = T_e(dT_e/dx)^{-1}$, and $L_u = c_s(du/dx)^{-1}$ are the density, temperature, and velocity gradient scale lengths, respectively. Note that in $CO_2$ driven plasmas, $v_0/v_e > 1$ so SBS is usually strongly driven.

We use Eq. (3) and the experimental measurements of Fig. 3, including a linear fit to the drift velocity, to evaluate $G$ versus $z$. To relate the calculated gain to the measured $\tilde{n}/n$ we need two things: (1) a relation between $\tilde{n}/n$ and the scattered light intensity, and (2) an estimate of the initial noise level from which the instability grows. We use the ion acoustic wave equation in one dimension to relate $\tilde{n}/n$ to the light energy [15]:

$$\frac{\partial^2\tilde{n}}{\partial t^2} - c_s^2\frac{\partial^2\tilde{n}}{\partial x^2} = \frac{Zn_e e^2}{mMc^2}\frac{\partial^2(\mathbf{E}_L \cdot \mathbf{E}_s)}{\partial x^2}. \quad (4)$$

For SBS, $E_{L,s} = E_{0_{L,s}} \sin(\omega_0 t \pm k_0 x)$ represent counterpropagating waves, where $E_L$ is the incident laser and $E_s$ is the backscattered light electric field. Substitution for $E_{L,s}$ and setting $\alpha = E_s/E_L$ gives

$$\partial^2\tilde{n}/\partial t^2 - c_s\partial^2\tilde{n}/\partial x^2 = 4k_0^2 c_s^2 n_e \alpha (v_0/v_e)^2 \cos 2k_0 x, \quad (5)$$

which has the solution

$$\tilde{n}/n_e = \alpha(v_0/v_e)^2 \cos(2k_0 x)(1 - \cos\omega_0 t). \quad (6)$$

For the purpose of comparison to experiment, we will use the maximum $\tilde{n}/n_e$ [$= \alpha(v_0/v_e)^2$] from the last equation. For the parameters of the experiment, $(v_0/v_e)^2 = 0.045$, which means that $\alpha^2 = I_{\tilde{n}}/I_L \leq 5 \times 10^{-5}$ from the measured fluctuation level. The scattered light intensity predicted by convective gain theory is $I_s = I_n e^G$, where $I_n$ is the initial scattered light noise level which can be either the thermal level of light (bremsstrahlung) or Thomson scattering of laser light by ion acoustic noise [16,17]. For $T_e = 1$ keV and $\lambda = 1.064$ nm, we calculate the thermal emission level to be $B(T) = 1 \times 10^{11}$ W cm$^{-2}$ sr$^{-1}$ cm$^{-1}$. The intensity scattered into a solid angle, $d\Omega$ of 0.2 sr, and a bandwidth of 1 nm, is $I_{\tilde{n}_T} = 2 \times 10^3$ Wcm$^{-2}$ or $I_{\tilde{n}_T}/I_L \simeq 2 \times 10^{-11}$. Thomson scattering from ion acoustic fluctuations, on the other hand, is estimated from [16] $I_{\tilde{n}_{ia}}/I_L \sim n_e \bar{\sigma} L_N$, where the scattering cross section $\bar{\sigma} \sim r_e^2$, to be $I_{\tilde{n}_{ia}}/I_L \sim 6 \times 10^{-7}$. Since our calculated gains are $<4$ so $e^G \leq 55$, we find a density fluctuation level similar to those seen with the Thomson scattering probe. The calculated and measured fluctuation profiles are compared in Fig. 5. We see that at earlier times ($t = 0.25$ and 0.5 ns) convective gain theory qualitatively agrees with the measured profile: both show increased fluctuations with increasing density. At $t = 0.75$ ns, the maximum density fluctuations occur at further distances from the target; this may be due to increased absorption of the laser light as the result of the increased plasma size. For the plasma parameters of this experiment, the absorption length is approximately 1 mm, which is comparable to the plasma size towards the end of the laser pulse.

Saturation of SBS at the laser intensity used in this experiment may not be important since other experiments have shown the backscattered energy to be below saturation [18] at $1 \times 10^{14}$ W/cm$^2$. Measured ion fluctuation profiles at incident energies of 25 and 75 J show a spatial behavior similar to that shown here. Interestingly, the largest density fluctuations occur at densities above $n_c/4$, i.e., at densities above which stimulated SRS can grow, which means that enhanced density fluctuations due to that instability do not lead, in this case, to a dominant SBS signal for densities below $n_c/4$ [19], although the larger ion fluctuations relative to the calculated growth at densities below $n_c/4$ seen in Fig. 5 may be due to enhanced noise. The relative importance of other parametric processes to seeding SBS probably depends on the driving laser wavelength and the density scale lengths which determine the relative thresholds of the underdense instabilities.

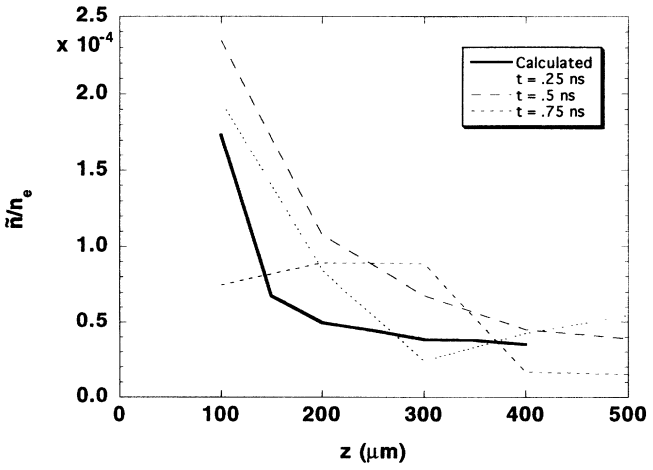


FIG. 5. The SBS density fluctuations determined from the measured scattered power versus axial position for three different times is compared to the density fluctuations calculated from convective gain theory and the measured hydrodynamic quantities of Fig. 3.

In conclusion, we have measured the ion fluctuation spatial profile in a plasma formed by laser irradiation of a solid target. Comparison of the profile to the results of convective gain theory calculated from measured hydrodynamic profiles shows good agreement. We have found that the thermal noise levels are far too low, given the convective gain that we calculate from the measured profiles, to account for the observed density fluctuations. Thomson scattering from ion acoustic fluctuations, however, give a good quantitative agreement with the observations.

We would like to thank Bill Cowens, Ray Gonzales, and Gary London for operating the Janus laser during the experiment. This work was performed under the auspices of the U. S. Department of Energy by the Lawrence Livermore National Laboratory under Contract No. W-7405-Eng-48.

[1] M. V. Goldman and D. F. DuBois, Annu. Phys. (N.Y.) **38**, 117 (1966).
[2] M. N. Rosenbluth, Phys. Rev. Lett. **29**, 565 (1972).
[3] C. S. Liu, M. N. Rosenbluth, and R. B. White, Phys. Rev. Lett. **31**, 697 (1973); Phys. Fluids **17**, 1211 (1974).
[4] J. F. Drake *et al.*, Phys. Fluids **17**, 778 (1974).
[5] D. W. Forslund, J. M. Kindel, and E. L. Lindman, Phys. Fluids **18**, 1002 (1975).
[6] D. E. Evans and J. Katzenstein, Rep. Prog. Phys. **32**, 207 (1969).
[7] J. Sheffield, *Plasma Scattering of Electromagnetic Radiation* (Academic, New York, 1975).
[8] J. E. Bernard and J. Meyer, Phys. Rev. Lett. **55**, 79 (1985); Phys. Fluids **29**, 2313 (1986).
[9] J. E. Bernard *et al.*, Phys. Fluids **30**, 11 (1987).
[10] P. E. Young *et al.*, Phys. Fluids B **3**, 1245 (1991).
[11] P. E. Young *et al.*, Phys. Fluids B **2**, 1907 (1990).
[12] P. E. Young, R. L. Berger, and K. G. Estabrook, Phys. Fluids B **4**, 2605 (1992).
[13] P. E. Young and K. G. Estabrook, Phys. Rev. E **49**, 5556 (1994).
[14] R. E. Slusher and C. M. Surko, Phys. Fluids **23**, 472 (1980).
[15] H. E. Huey *et al.*, Phys. Rev. Lett. **45**, 795 (1980).
[16] C. J. Randall, J. R. Albritton, and J. J. Thomson, Phys. Fluids **24**, 1474 (1981).
[17] R. L. Berger, E. A. Williams, and K. G. Estabrook, Phys. Fluids **1**, 414 (1989).
[18] P. E. Young, Phys. Fluids B **5**, 2265 (1993).
[19] H. A. Baldis *et al.*, Phys. Fluids B **5**, 3319 (1993).

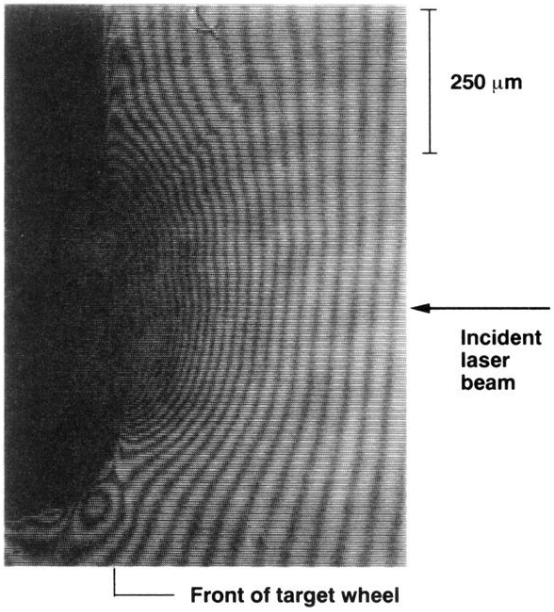


FIG. 4. The interferograms are recorded at the peak of the laser pulse by a 30 ps, 0.35 $\mu$m probe pulse. The shadow of the target wheel is shown. The Thomson scattered signal for the $T_e$ measurement is collected by a lens located below the target wheel in this picture.